171

• Institute of Applied Mechanics,
• Institute of Mechanics
Vietnamese Academy of Science and Technology
• Laboratoire de Mécanique des Solides
Ecole Polytechnique, Paris

with the participation of Vietnam Society of Mathematics and Vietnam Association of Mechanics

International Conference on

NONLINEAR ANALYSIS & ENGINEERING MECHANICS TODAY

*Dedicated to **Prof. Dang Dinh Ang** on the occasion of his 80th birthday*

PROCEEDINGS

Editors : **Nguyen Dung**
Nguyen Quoc Son

PUBLISHING HOUSE FOR SIENCE AND TECHNOLOGY

Yield Design Theory applied to the Determination of the Seismic Bearing Capacity of Surface Footings

J. Salençon, C. Chatzigogos, A. Pecker

LMS, UMR 7649, École Polytechnique, F-91128 Palaiseau cedex, France
salencon@lms.polytechnique.fr

Abstract

The kinematic approach of the Yield design theory, as developed during the past decades, provides a way of approach to the stability analysis of civil engineering structures under seismic conditions. As an example new results for the seismic bearing capacity of circular footings resting on a purely cohesive soil are presented here in the form of surfaces in the space of the loading parameters of the footing for a range of values of the horizontal inertia forces acting in the soil. Practical applications of these results concern the safety coefficient to be applied on the vertical load when designing seismic foundations.

A survey of the Yield design theory

Historical landmarks

The Yield design theory originates in the celebrated Coulomb's Essay published in 1773 where the stability or the resistance of various structures is assessed. A famous and usual reference is also the analysis of the resistance to bending of a cantilever beam by Galileo (1638). As far as the constituent materials are concerned, these analyses have in common that they only rely on one data, namely the resistance of the material defined once for all through a strength criterion on the stress state at any point of the structure. Similar approaches are encountered in many branches of civil or construction engineering with some famous methods of stability analysis in soil mechanics or the Johansen yield line method for the analysis of the bearing capacity of reinforced concrete slabs. Through a simple application of convex analysis a comprehensive theory can be formulated which covers all already existing methods and makes the dialogue between them easier. A brief outline of this theory is now given in order to introduce its application to a footing bearing capacity problem in the earthquake engineering context.

An outline of the Yield design theory

The Yield design theory [17] [18] aims at estimating the ***extreme loads*** that can be supported by a structure once three pieces of information are available, namely: as regards the structure itself, its geometry and the loading process it is submitted to and, as regards the constituent materials, their strength criteria, whatever the physical phenomena they are related to. Since it does not need incorporating any data about the constitutive law of the materials before and at failure, it should be kept in mind that the obtained results are but upper bound estimates for the actual ultimate loads and also that no information can be obtained regarding the displacements. The theory will be formulated within the 3D-continuum mechanics framework. The geometry being given, the generic notations Ω and $\partial\Omega$ will be used for the volume and the boundary of the system. The quasi-static loading mode of the system is described through a multi parameter loading vector $\underline{Q}$ with components Q_i and the associated dual kinematic parameters $\hat{\dot{q}}_i$ defining the virtual kinematic vector $\underline{\hat{\dot{q}}}$. The principle of virtual rates of work (*viz.* [19]) thus writes in the form:

$$\forall \underline{\underline{\sigma}} \text{ statically admissible with } \underline{Q},\ \forall \underline{\hat{U}} \text{ kinematically admissible with } \underline{\hat{\dot{q}}},$$

$$\int_{\Omega} \underline{\underline{\sigma}} : \underline{\underline{\hat{d}}} \, \mathrm{d}\Omega + \int_{\Sigma_{\underline{\hat{U}}}} \underline{n} \cdot \underline{\underline{\sigma}} \cdot [\![\underline{\hat{U}}]\!] \, \mathrm{d}\Sigma_{\underline{\hat{U}}} = \underline{Q} \cdot \underline{\hat{\dot{q}}} \tag{1}$$

with

$$\underline{\underline{\sigma}} \mapsto \underline{Q} \text{ and } \underline{\hat{U}} \mapsto \underline{\hat{\dot{q}}} \text{ linear} \tag{2}$$

where the symbol " : "denotes the double contracted product and "." the dot product. $\underline{\underline{\sigma}}$ stands for the Cauchy stress tensor field, $\underline{\underline{\hat{d}}}$ for the virtual strain rate tensor field derived from the virtual velocity field $\underline{\hat{U}}$ and $\Sigma_{\underline{\hat{U}}}$ for the virtual velocity jump surfaces.

The same description is adopted in the case of a dynamic loading treated as a quasi-static phenomenon by incorporating the corresponding given inertia forces within the applied external forces. The resistance of the constituent material is defined at any point of the system through a convex strength criterion to be satisfied by the stress state. Homogeneity is not assumed and the term constituent material is a generic one for all the material constituting the system, including the interfaces between different elements.

The question to be answered is to determine the loads $\underline{Q}$ that can be supported by the system under the specified strength conditions. As an answer it is clear that mathematical compatibility at any point of the system between the equilibrium equations and the material resistance conditions is necessary for a load to be supported: such loads generate the convex domain K of the ***potentially safe*** loads in the $\{\underline{Q}\}$ vector space. The boundary of K defines the ***extreme loads*** of the system. Any stress field in equilibrium with a load $\underline{Q}$ that complies with the strength criterion is sufficient to prove that $\underline{Q} \in K$. This is the basis of the ***internal approach*** or lower bound approach of the extreme loads. As already explained, strictly speaking, the extreme loads are but upper bound estimates of the actual ultimate loads of the system. However it must be emphasized that the extreme loads being independent of the material behaviour characteristics other than the strength criteria and of the loading paths and loading history, are valid whatever these data. After being assessed and through convenient safety factors, they provide a reliable theoretical bench mark for practical applications.

It turns out that the internal approach, since it requires the construction of stress fields that satisfy the above mentioned conditions is often difficult to implement. Fortunately, dualization through the principle of virtual rates of work (1) (2) leads to an external approach based upon the construction of kinematically admissible virtual velocity fields. The details of the related reasoning can be found in [18] and just the main features will be recalled here. The key idea is that the material resistance may be equivalently defined through the strength criteria on the stress tensor as indicated above or through the associated $\pi-$functions of the strain rate $\underline{\underline{\hat{d}}}$: denoting generically by G the domain of resistance on $\underline{\underline{\sigma}}$ defined at a point of the system, the corresponding $\pi-$function is just the "support function"

$$\pi(\underline{\underline{\hat{d}}}) = \mathrm{Sup}\left\{\underline{\underline{\sigma}}':\underline{\underline{\hat{d}}} \,\middle|\, \underline{\underline{\sigma}}' \in G\right\} \tag{3}$$

from which we derive

$$\pi(\underline{n},[\![\underline{\hat{U}}]\!]) = \mathrm{Sup}\left\{\underline{n}.\underline{\underline{\sigma}}'.[\![\underline{\hat{U}}]\!] \,\middle|\, \underline{\underline{\sigma}}' \in G\right\}. \tag{4}$$

For obvious reasons the $\pi-$functions are called the maximum resisting rate of work densities. From the definition of K and through (1) (2), the fundamental inequality of the external approach is obtained in the form:

$$\forall \underline{Q} \in K, \forall \underline{\hat{U}} \text{ kinematically admissible virtual velocity field,} \tag{5}$$

$$\underline{Q}.\underline{\hat{q}} \leq \int_{\Omega} \pi(\underline{\underline{\hat{d}}})\,\mathrm{d}\Omega + \int_{\Sigma_{\underline{\hat{U}}}} \pi(\underline{n},[\![\underline{\hat{U}}]\!])\,\mathrm{d}\Sigma_{\underline{\hat{U}}}\,. \tag{6}$$

The right hand side of (6) is called maximum resisting rate of work in the virtual velocity field $\underline{\hat{U}}$:

$$P_{\mathrm{rm}}(\underline{\hat{U}}) = \int_{\Omega} \pi(\underline{\underline{\hat{d}}})\,\mathrm{d}\Omega + \int_{\Sigma_{\underline{\hat{U}}}} \pi(\underline{n},[\![\underline{\hat{U}}]\!])\,\mathrm{d}\Sigma_{\underline{\hat{U}}} \tag{7}$$

while the left hand side of (6) is just the rate of work of all the external forces $P_{\mathrm{e}}(\underline{Q},\underline{\hat{U}})$. It follows from (6) (7) that the construction of any kinematically admissible (k.a.) virtual velocity field $\underline{\hat{U}}$ yields an external approach of the boundary of K :

$$\forall \underline{\hat{U}} \text{ k. a., } K \subset \left\{P_{\mathrm{e}}(\underline{Q},\underline{\hat{U}}) - P_{\mathrm{rm}}(\underline{\hat{U}}) \leq 0\right\}. \tag{8}$$

The two approaches are schematically presented in Figure 1. Important points regarding the external approach are:

- Tables giving the expressions of the $\pi-$functions for usually encountered criteria are available (*viz.* [17], [20]);

- For a given G the values of the $\pi-$functions are either finite or infinite depending on the values of the arguments $\underline{\underline{\hat{d}}}$ and $(\underline{n},[[\underline{\hat{U}}]])$;
- For the approach to be efficient k. a. $\underline{\hat{U}}$ must be chosen in order that the values of the $\pi-$functions remain finite everywhere in Ω;
- The latter condition has no relationship whatsoever with a constitutive law.

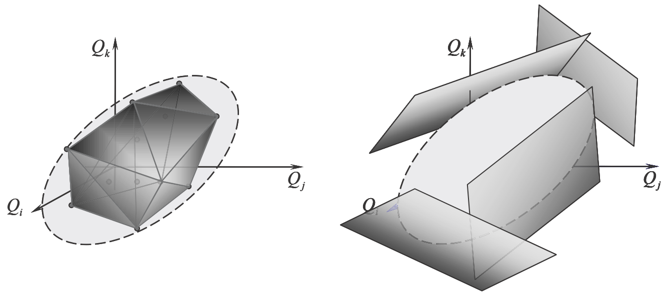

Figure 1.Internal and external approaches of the domain of potentially safe loads

Seismic bearing capacity of a circular footing on a purely cohesive soil

Problem motivation

The problem under consideration arises from a series of field observations after several major earthquakes within the last twenty five years, which revealed a particular type of foundation failure without the presence of liquefaction in the supporting soil layers: large permanent rotations were observed at the foundation level together with a zone of detachment at the soil-foundation interface and the development of a failure mechanism within the soil volume (*viz*. [10]). The same failure mechanism was also identified experimentally [9] [26].

From a theoretical point of view, one initial approach to the problem of the seismic bearing capacity is to work within the classical framework of Terzaghi's bearing capacity formula, modifying the bearing capacity factors N_c, N_q, N_γ in order to account for the effect of the inertia forces within the soil volume during the seismic excitation, while applying appropriate correction factors for the load eccentricity and inclination [6] [16] [25]. A second approach represents the seismic bearing capacity of the foundation system as an "ultimate surface" in the space of the loading parameters of the footing as a function of the intensity of the horizontal inertia forces in the soil volume [11] [12] [13] [22] [23]. The results so-obtained were incorporated in the European norms for earthquake resistant design of civil engineering structures [5].

The present study aims at extending the analysis to the seismic bearing capacity of a shallow circular footing resting on the surface of a purely cohesive soil layer.

Definition of the seismic bearing capacity problem

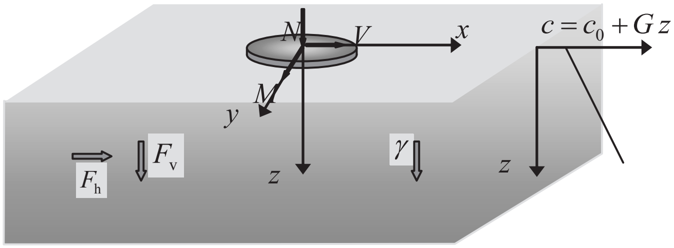

Figure 2. Circular shallow foundation under seismic loading on a purely cohesive soil

A rigid circular footing with radius r resting on a purely cohesive soil half space is considered (Figure 2). The resistance of the constituent soil is described by the Tresca criterion with a cohesion c depending linearly on the depth (9) with c_0 the surface cohesion and G the vertical cohesion gradient:

$$c = c_0 + G z \,. \tag{9}$$

In order to assess the importance of the corresponding assumption, two extreme cases are considered, namely, the classical Tresca criterion (10) and the Tresca criterion with zero resistance to tension (11):

$$f\left(\underline{\underline{\sigma}}\right) = \left|\sigma_1 - \sigma_3\right| - 2c \leq 0 \,, \tag{10}$$

$$f\left(\underline{\underline{\sigma}}\right) = \sup\left\{\left|\sigma_1 - \sigma_3\right| - 2c,\ \sigma_1\right\} \leq 0 \,, \tag{11}$$

with σ_1 and σ_3 the major and minor principal stresses respectively (tensile stresses positive).

The soil-footing interface is also considered as purely cohesive and its resistance is modelled by the Tresca criterion with no tensile resistance (zero tension “cut-off”). This is a deliberate choice in order to allow for the potential creation of a zone of detachment between the footing and the soil, an essential characteristic of observed seismic bearing capacity failure. The interface cohesion is considered equal to c_0.

$$f(\sigma, \tau) = \sup\left\{\left|\tau\right| - c_0, \sigma\right\} \leq 0 \,. \tag{12}$$

The quasi-static loading mode of the system is defined by means of the wrench of external forces acting on the footing due to the weight and to the inertial response of the superstructure (including the footing itself), of the unit weight of the soil and of the intensity of the inertia forces developing within the soil mass.

Following common practice, this intensity is assumed to be uniform throughout the soil mass with vertical and horizontal components F_{v} and F_{h} respectively. The validity of this assumption has already been discussed by various authors (*e.g.* [13] suggested that, denoting by d and D respectively the failure mechanism thickness and the depth of the soil layer, the following condition should be satisfied: *d/D*<10). From now on the vertical component F_{v} will be added to the unit weight of the soil and give rise to the modified unit weight:

$$\underline{\gamma}^* = \underline{\gamma} + \underline{F}_{\text{v}} = \gamma^* \underline{e}_z \,, \tag{13}$$

with $\underline{e}_z$ the unit vector in the descending vertical direction.

Due to the origin of the external loads acting on the superstructure and on the foundation, it is also assumed that the horizontal component V of the resultant force of the wrench is collinear with the horizontal inertia force F_{h} in the soil along the x axis, and that the horizontal overturning moment M at the centre of the footing is oriented around the y axis, perpendicular to that direction. As a matter of fact, this assumption is rigorously valid when dealing with the excitation of a single-degree-of-freedom (SDOF) superstructure and under specific conditions in the multi-degree-of-freedom case.

Relevant variables for the seismic bearing capacity problem

The determination of the bearing capacity of the foundation under the conditions specified here above is based upon the Theory of yield design. Concerning the influence of the modified unit weight on the extreme loads, it has been shown (*viz.* [17]) that, for the classical Tresca criterion, the unit weight has no influence on the value of the extreme loads supported by the footing. For the case of the Tresca criterion with no resistance to tension, the result remains true if $\gamma^* \geq 0$, which is true in the usual cases of seismic excitations. Therefore, γ^* will no longer appear in the problem loading parameters.

Dimensionless parameters

The vertical component of resultant force acting on the footing is denoted by N. The horizontal component F_{h} is defined from a horizontal acceleration a_{h} characteristic of the examined earthquake, which can be for instance the peak ground horizontal acceleration (PGHA):

$$F_{\text{h}} = \rho a_{\text{h}} \tag{14}$$

with ρ the mass density of the soil.

The vector $\underline{Q}$ representing the loading parameters of the system is written:

$$\underline{Q} = (N, V, M, F_{\mathrm{h}}) \tag{15}$$

and the strength parameters are c_0 and G.

When presenting the results, dimensionless parameters will be introduced:

$$\boldsymbol{N} = \frac{N}{\pi c_0 r^2}, \boldsymbol{V} = \frac{V}{\pi c_0 r^2}, \boldsymbol{M} = \frac{M}{2\pi c_0 r^3}, \boldsymbol{F}_{\mathrm{h}} = \frac{\rho r a_{\mathrm{h}}}{\pi c_0}, \boldsymbol{k} = \frac{rG}{c_0}. \tag{16}$$

The parameter $\boldsymbol{k}$ expresses the degree of heterogeneity in the system. For a homogeneous soil layer, $\boldsymbol{k} = 0$. Common values of *r*, *G* and C_0 give rise to $\boldsymbol{k}$ smaller or equal to approximately **2**.

Solution procedure

The kinematic approach of the Yield design theory is implemented on this problem through the construction of virtual k.a. velocity fields in the whole system, that are relevant for the strength criteria under concern by referring to the $\pi -$functions corresponding to (10-12):

- Classical Tresca criterion (10)

$$\begin{aligned}
&\pi(\underline{\underline{\hat{d}}}) = +\infty \text{ if } \operatorname{tr}(\underline{\underline{\hat{d}}}) \neq 0, \\
&\pi(\underline{\underline{\hat{d}}}) = c(\left|\hat{d}_1\right| + \left|\hat{d}_2\right| + \left|\hat{d}_3\right|) \text{ if } \operatorname{tr}(\underline{\underline{\hat{d}}}) = 0, \\
&\pi(\underline{n}, [\![\underline{\hat{U}}]\!]) = +\infty \text{ if } [\![\underline{\hat{U}}]\!].\underline{n} \neq 0, \\
&\pi(\underline{n}, [\![\underline{\hat{U}}]\!]) = c\left|[\![\underline{\hat{U}}]\!]\right| \text{ if } [\![\underline{\hat{U}}]\!].\underline{n} = 0.
\end{aligned} \tag{17}$$

- Tresca criterion with zero tension cut-off (11)

$$\begin{aligned}
&\pi(\underline{\underline{\hat{d}}}) = +\infty \text{ if } \operatorname{tr}(\underline{\underline{\hat{d}}}) < 0, \\
&\pi(\underline{\underline{\hat{d}}}) = c(\left|\hat{d}_1\right| + \left|\hat{d}_2\right| + \left|\hat{d}_3\right| - \operatorname{tr}(\underline{\underline{\hat{d}}})) \text{ if } \operatorname{tr}(\underline{\underline{\hat{d}}}) \geq 0, \\
&\pi(\underline{n}, [\![\underline{\hat{U}}]\!]) = +\infty \text{ if } [\![\underline{\hat{U}}]\!].\underline{n} < 0, \\
&\pi(\underline{n}, [\![\underline{\hat{U}}]\!]) = c\left|[\![\underline{\hat{U}}]\!] - [\![\underline{\hat{U}}]\!].\underline{n}\right| \text{ if } [\![\underline{\hat{U}}]\!].\underline{n} \geq 0.
\end{aligned} \tag{18}$$

- Tresca criterion for the interface without resistance to tension (12)

$$\pi(\underline{n},[\![\underline{\hat{U}}]\!]) = +\infty \text{ if } [\![\underline{\hat{U}}]\!].\underline{n} < 0\,,$$
$$\pi(\underline{n},[\![\underline{\hat{U}}]\!]) = c\left|[\![\underline{\hat{U}}]\!] - ([\![\underline{\hat{U}}]\!].\underline{n}).\underline{n}\right| \text{ if } [\![\underline{\hat{U}}]\!].\underline{n} \geq 0\,. \tag{19}$$

It follows obviously that a relevant virtual velocity field for the classical Tresca criterion is also relevant for the Tresca criterion without tensile strength, but not vice-versa. Attention must be paid also to (19) as it shows that a non-zero maximum resisting rate of work is obtained even when a detachment between the footing and the soil is induced by the virtual velocity field.

Since the circular footing is assumed to be perfectly rigid, any virtual k.a velocity field $\underline{\hat{U}}$ must comply with a rigid body motion of the footing as a boundary condition. For the planar velocity fields that will be considered hereafter, assuming $\hat{U}_y = 0$, such a rigid body motion is defined by the virtual rate of rotation $\hat{\omega}$ and the two components $\hat{U}_{O,x}, \hat{U}_{O,z}$ of the virtual velocity of the center O of the footing. Consequently the rate of work of the external forces is written:

$$\underline{\underline{Q}}.\underline{\underline{\hat{q}}} = N\hat{U}_{O,z} + V\hat{U}_{O,x} + M\,\hat{\omega} + F_{\mathrm{h}}\int_{\Omega}\underline{\hat{U}}.\underline{e}_x\,\mathrm{d}\Omega\,. \tag{20}$$

Three classes of virtual k.a. velocity fields $\underline{\hat{U}}$ have been examined, which are derived from plane strain potential failure mechanisms used to determine the seismic bearing capacity of strip footings. Completely described in [2] [3], these planar and non-plane strain virtual velocity fields are parallel to Oxz and depend on the three coordinates. They are relevant for the strength criteria (10-12) since they are isochoric everywhere in Ω: $\mathrm{tr}(\underline{\underline{\hat{d}}}) = 0$, $[\![\underline{\hat{U}}]\!].\underline{n} = 0$, but for the interface where virtual uplift of the footing with respect to the soil surface may occur $[\![\underline{\hat{U}}]\!].\underline{n} \geq 0$. In order to implement the external approach through (8) $P_{\mathrm{rm}}(\underline{\hat{U}})$ must be computed, which implies deriving $\underline{\underline{\hat{d}}}$ from $\underline{\hat{U}}$, a tedious task until it was drastically simplified by Puzrin and Randolph [14] [15]in a method based upon the use of wisely chosen curvilinear coordinates.

- ***"Translational"*** virtual failure mechanisms were originally proposed in plane strain [7] for the indentation by a rigid punch submitted to an inclined load; the extension to a rigid circular footing was given by Puzrin and Randolph by considering that the width of the mechanism in a cross-section by a vertical plane is proportional to the width of the footing in the same cross-section (Figure 3). The footing translates with a virtual velocity $\underline{\hat{U}}_0$ which propagates with a constant magnitude along the streamlines of the mechanism.

The shape of each virtual failure mechanism is defined by the two angles: $0 < \delta < \pi/2$, $0 < \varepsilon < \pi/2$. The mechanisms exhibit three zones within the soil mass, presented in Figure 2. Zones 1 and 3 translate rigidly while zone 2 is a region where non-plane shear strain rate is developed. Contributions to the maximum resisting rate of work for this class are developed within the volume of zone 2 and along the velocity jump surface in the soil. These virtual mechanisms involve no rotation of the footing: the upper bound estimates they provide through (8) do not involve the moment M.

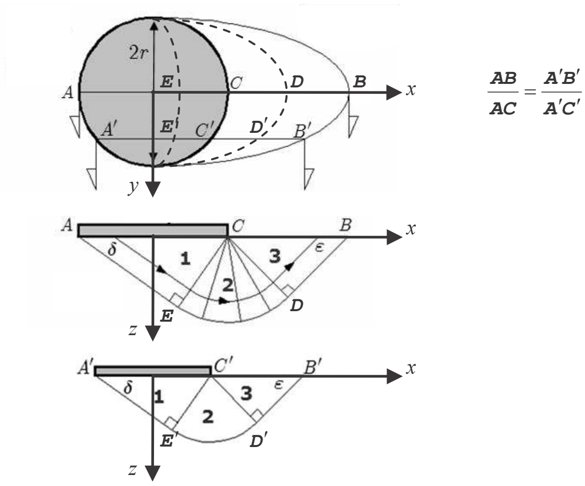

Figure 3. Translational virtual failure mechanism

- ***"Purely rotational"*** virtual failure mechanisms are adapted from the plane strain version studied in [22] [23] [24]. The rigid circular footing is considered to rotate rigidly around an axis parallel to Oy and induces rigid rotational failure of the soil below with a virtual angular velocity $\hat{\omega}$ (Figure 4). Each mechanism is defined by the geometrical parameters κ and λ. For $1 < \lambda < 2$, there is no uplift of the footing with respect to the soil surface and the maximum resisting rate of work is only produced along the velocity jump surface within the soil volume. For $0 < \lambda < 1$, uplift of the footing with respect to the soil surface takes place in the zone of soil-footing detachment where consequently a fraction of the maximum resisting rate of work is developed.

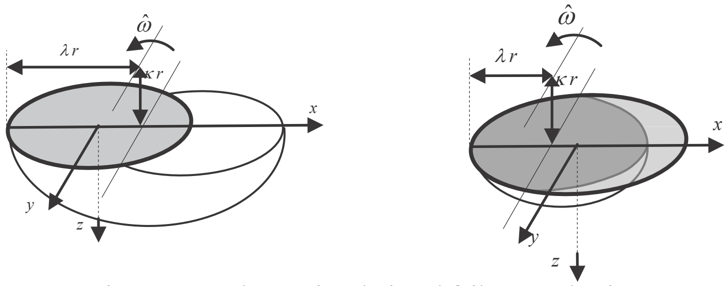

Figure 4. Purely rotational virtual failure mechanism

- ***"Shear-rotational"*** virtual failure mechanisms follow a pattern derived from the plane-strain virtual velocity field originally proposed by Brinch Hansen 0 for the study of active earth pressures.

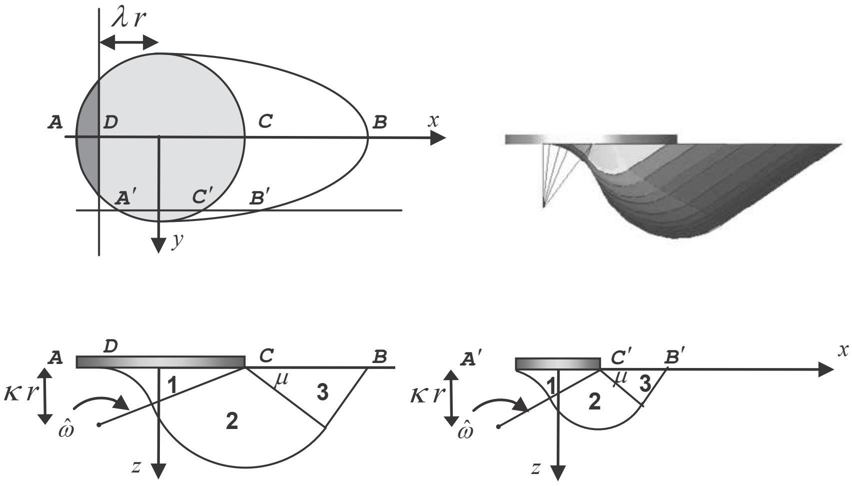

Figure 5. Shear-rotational virtual failure mechanism

Rigid body rotation of the footing around an axis of rotation parallel to Oy located within the soil mass induces the development of non planar shear strain rate in the zones 2 and 3 within the soil volume The mechanisms depend on the three geometrical parameters κ, λ, μ and three distinct configurations are obtained depending on the position of the axis of rotation with respect to the footing: without uplift of the footing with respect to the soil surface or with a small or large zone of detachment; contributions to the maximum resisting rate of work are developed within the soil volume in zones 2 and 3, along the velocity jump surface in the soil mass and on the zone of soil-footing detachment, if any.

Results

Implementing the external approach through (8), the rate of work of the external forces is given by (20) and the maximum resisting rate of work $P_{\mathrm{rm}}(\underline{\hat{U}})$ is computed through (7) with the relevant expressions for $\pi(\underline{\underline{\hat{d}}})$ and $\pi(\underline{n},[[\underline{\hat{U}}]])$. Looking for optimal upper bounds for the ultimate loads supported by the system, an optimization procedure is performed over each separate geometrical configuration of the considered classes of virtual mechanisms: in each case, it reduces to minimizing a nonlinear objective function with respect to the parameters of the geometric configuration. This problem was solved on a commercial platform for scientific computing with an algorithm using a robust interior trust region approach [4]. The following results were obtained.

- ***Critical value of*** $\boldsymbol{F}_{\mathrm{h}}$. Failure of the system may occur just due to the action of the soil inertia forces when $\boldsymbol{F}_{\mathrm{h}}$ exceeds a critical value while the other loading parameters are zero: $\boldsymbol{N}=0, \boldsymbol{V}=0, \boldsymbol{M}=0$. Table 1 summarizes the calculated values of critical $\boldsymbol{F}_{\mathrm{h}}$ as a function of $\boldsymbol{k}$ for the classes of mechanisms examined. It shows an important increase of the critical value with increasing $\boldsymbol{k}$. The minimum value $\boldsymbol{F}_{\mathrm{h}}=0.66$ is obtained through a shear-rotational virtual failure mechanism. For homogeneous soils and usual values of the other parameters, this value corresponds to a very strong earthquake: *e.g.* $a_{\mathrm{h}}=10\,\mathrm{m/sec}^2 \cong g$ for $r=4\,\mathrm{m}, c_0=40\,\mathrm{kPa}, \rho=20\,\mathrm{kN/m}^3$ and this value is obtained for a mechanism with very large dimensions with respect to the footing width that has no physical meaning whatsoever.

Class of mechanisms	**critical value of $\boldsymbol{F}_{\mathrm{h}}$**			
	$\boldsymbol{k}=\mathbf{0}$	$\boldsymbol{k}=\mathbf{0.5}$	$\boldsymbol{k}=\mathbf{1}$	$\boldsymbol{k}=\mathbf{3}$
Translational	1.32	1.80	2.29	4.05
Purely rotational	0.99	1.28	1.54	2.45
Shear rotational	**0.66**	**0.90**	**1.15**	**2.03**
MINIMUM	**0.66**	**0.90**	**1.15**	**2.03**

Table 1. Values of the critical value of $\boldsymbol{F}_{\mathrm{h}}$ as a function of $\boldsymbol{k}$.

- ***Presentation of the results.*** The upper bounds for the ultimate loads supported by the foundation are represented as surfaces in the space of the loading parameters $(\boldsymbol{N}, \boldsymbol{V}, \boldsymbol{M})$ for different values of $\boldsymbol{F}_{\mathrm{h}}$ and $\boldsymbol{k}$ by means of the sections of those surfaces which represent the interaction diagrams: these curves represent the bounds for the ultimate combinations of the loading parameters and indicate the class of mechanisms from which each bound is obtained. In the following, the results refer to the more realistic Tresca criterion with a zero tension "cut-off" for the soil strength. For brevity sake, only some significant results will be reported here; a comprehensive and commented report may be found in [2] [3].

- ***Interaction diagram* (*N, V, M* = 0, *F*$_{\mathrm{h}}$)**

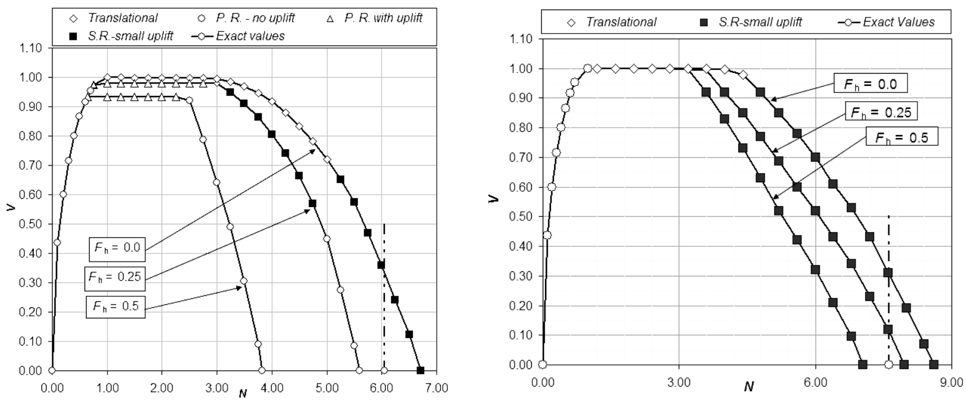

Figure 6. Tresca criterion with zero tension "cut-off": Interaction diagram (***N***, ***V***, ***M*** = 0, ***F***$_{\mathrm{h}}$) for ***k*** = 0 and ***k***= 1

The diagrams in Figure 6 present the relation between the ultimate horizontal and vertical force for $\boldsymbol{k} = 0$ and $\boldsymbol{k} = 1$, for three different values of $\boldsymbol{F}_{\mathrm{h}}$. The maximum value for $\boldsymbol{V}$ is 1, corresponding to a translational mechanism of failure by pure sliding along the soil-footing interface when $\boldsymbol{F}_{\mathrm{h}} = 0$. It is also interesting to note that for $\boldsymbol{F}_{\mathrm{h}} > 0$ the purely rotational virtual mechanism gives a better upper bound than the pure sliding one: although the depth of this mechanism is relatively small, so that it is very close to a pure sliding, it incorporates a contribution of $\boldsymbol{F}_{\mathrm{h}}$ to the rate of work of the external forces. This phenomenon is less pronounced for larger values of $\boldsymbol{k}$ as revealed by the diagram for $\boldsymbol{k} = 1$. For practical applications it is worth noting that, both for $\boldsymbol{k} = 0$ and for $\boldsymbol{k} = 1$, the effect of $\boldsymbol{F}_{\mathrm{h}}$ remains negligible as long as $\boldsymbol{N}^{0}_{\max} / \boldsymbol{N} > 2.5$, where $\boldsymbol{N}^{0}_{\max}$ denotes the known exact value of the maximal vertical force supported by the footing with $\boldsymbol{F}_{\mathrm{h}} = 0$ (*viz.*

[21]). As N increases so does the negative effect of a high value of F_h, especially when $N_{max}^0 / N < 2$ but it is observed that it is less pronounced for $k = 1$ than for $k = 0$: a favourable effect of the vertical cohesion gradient.

- ***Interaction diagram* (*N, V*= 0, *M*, F_h)**

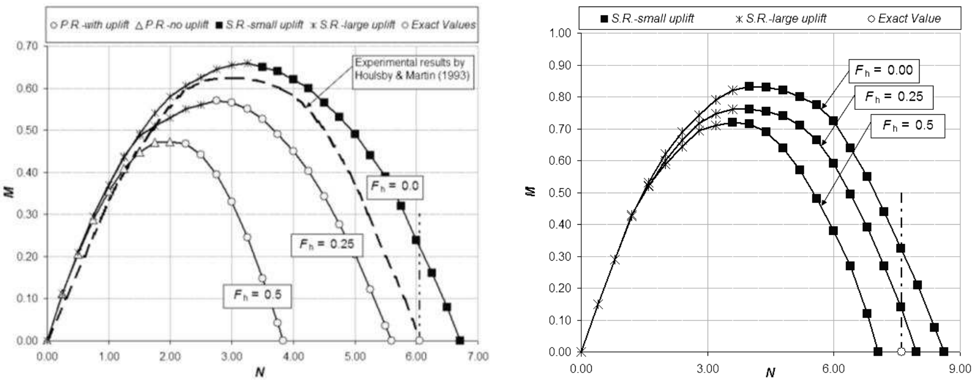

Figure 7. Tresca criterion with zero tension "cut-off": Interaction diagram (***N***, ***V*** = 0, ***M***, F_h) for ***k*** = 0 & ***k***= 1, and experimental results by Houlsby & Martin [8]

Figure 7 presents the optimal upper bounds for the ultimate combinations of M and N obtained with $V = 0$, for $k = 0$ and $k = 1$. Experimental data in the case $k = 0$, $F_h = 0$ from the paper by Houlsby & Martin [8] are plotted for comparison. It comes out that the upper bounds are satisfactory, from a practical point of view, and that the difference is larger for the larger values of N that correspond to quasi axisymmetrical loading configurations, which the considered unilateral virtual failure mechanisms are not well suited to. For small values of N, the optimal upper bounds are obtained by mechanisms with a significant zone of detachment of the footing, which is not the case as N increases. The effect of F_h follows the same behaviour as in Figure 6, which, from a practical point of view, enforces the conclusion from this observation that a factor of safety against permanent loads $N_{max}^0 / N > 2.5$ can guarantee that the effect of soil inertia forces is negligible, even for very strong earthquakes. Such conclusions are in agreement with observations of real foundation bearing capacity failures, mainly after the Guerrero-Michoacán earthquake (Mexico, 1985) as presented in [10].

- ***Interaction diagram* (*N=const., V, M, F*$_h$)**

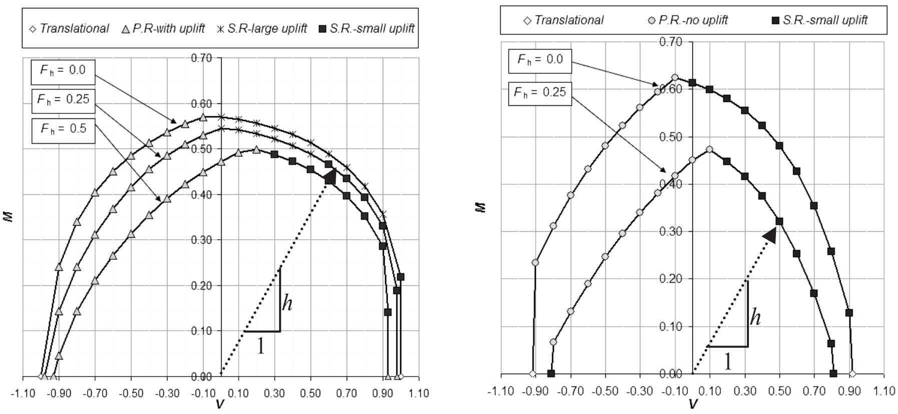

Figure 7. Tresca criterion with zero tension “cut-off”: (***N=const***, ***V***, ***M***, ***F***$_h$) Interaction diagram for $\boldsymbol{k} = 0$, $\boldsymbol{N}^0_{\max} / \boldsymbol{N} > 3$ and $\boldsymbol{N}^0_{\max} / \boldsymbol{N} > 3/2$; ultimate loading paths for $\boldsymbol{F}_h = 0{,}25$ in a SDOF superstructure

The interaction diagrams between the ultimate values of $\boldsymbol{V}$ and $\boldsymbol{M}$ for fixed values of the vertical force $\boldsymbol{N}$ are shown in Figure 8 for $\boldsymbol{k} = 0$ in the two cases $\boldsymbol{N}^0_{\max} / \boldsymbol{N} = 3$ corresponding to a proper foundation design and $\boldsymbol{N}^0_{\max} / \boldsymbol{N} = 1.5$ corresponding to a non conservative design. These diagrams can be used for practical applications when a relationship between the resultant moment and the horizontal force (base shear force) on the footing is known from the geometrical and rigidity characteristics of the superstructure Such a relationship defines a loading path in the $(\boldsymbol{V}, \boldsymbol{M})$ plane allowing for the determination of the ultimate combination of $\boldsymbol{V}$ and $\boldsymbol{M}$ for given $\boldsymbol{N}$ and $\boldsymbol{F}_h$. Such loading paths are presented in Figure 8 where the two diagrams highlight the significant decrease of the bearing capacity with increasing $\boldsymbol{F}_h$ for $\boldsymbol{N}^0_{\max} / \boldsymbol{N} = 1.5$. Even for $\boldsymbol{V} = 0$, $\boldsymbol{M} = 0$, a value $\boldsymbol{F}_h = 0.5$ causes the collapse of the footing.

Practical implementation

As explained earlier the Eurocode 8 expression [5] for the seismic bearing capacity of shallow foundations is only valid for strip footings resting on homogeneous soils, either purely cohesive or purely frictional. The present study makes it possible to propose a modified version of those rules for shallow circular footings on a purely cohesive soil with a vertical cohesion gradient. The corresponding expression is exposed and discussed in [2] [3]. As far as the design principles are concerned, it should be retained that the effect of the horizontal inertia forces in the soil volume is, in general, negligible as long as the vertical force on the footing remains smaller than one third of its static bearing capacity.

As a conclusion

Seismic solicitations must now often be taken into account when designing private or industrial buildings or structures such as bridges, dams, nuclear plants, *etc.* We have briefly outlined how such a problem can be thoroughly studied from the theoretical point of view through the Yield design approach up to the writing of new international design codes. This is just an example to enhance how, as a theoretical basis, the Yield design theory is a corner stone of Ultimate limit state design (ULSD).

References

[1] BRINCH HANSEN, J. *Earth Pressure Calculation.* The Danish Technical Press - Institution of Danish Civil Engineers, Copenhagen, (1953).

[2] CHATZIGOGOS, C. *PhD Thesis* (2007).

[3] CHATZIGOGOS, C., PECKER, A., SALENÇON, J. Seismic bearing capacity of a circular footing on a heterogeneous cohesive soil. Submitted to *Soils and Foundations.*

[4] COLEMAN, T., F., LI, Y. An interior trust region approach for nonlinear minimization subject to bounds. *SIAM Journal on Optimization,* **6,** 2, pp. 418-445 (1996).

[5] EUROCODE 8. *Partie 5*, *Conception et dimensionnement des structures pour leur résistance aux séismes.* Commission Européenne de Normalisation. prENV 1998.

[6] FISHMAN, K. L., RICHARDS, R., YAO, D. Inclination factors for seismic bearing capacity. *Journal of Geotechnical and Geoenvironmental Engineering ASCE,* **129**, 9, pp. 861-865 (2003).

[7] GREEN, A., P. The plastic yielding of metal junctions due to combined shear and pressure. *Journal of Mechanics and Physics of Solids* **2,** 3, pp. 197 – 211 (1954).

[8] HOULSBY, G., T., MARTIN, C., M. Modelling of the behaviour of foundations of jack-up units on clay. *Predictive Soil Mechanics.* Thomas Telford, London, pp. 339 – 358 (1993).

[9] KNAPPETT, J., A., HAIGH, S., K., MADABHUSHI, S., P., G. Mechanisms of failure for shallow foundations under earthquake loading. *Soil Dynamics and Earthquake Engineering,* **26**, 2-4, pp. 91-102 (2006).

[10] MENDOZA, M. J., AUVINET, G. The Mexico earthquake of September 19, 1985 - Behavior of building foundations in Mexico City. *Earthquake Spectra,* **4***,* 4, pp. 835-852 (1988).
[11] PAOLUCCI, R., PECKER, A**.** Soil Inertia Effects on the Bearing Capacity of rectangular Foundations on cohesive Soils. *Engineering Structures,* **19**, 8, pp. 637-643 (1997).
[12] PAOLUCCI, R., PECKER, A. Seismic Bearing Capacity of Shallow Strip Foundations on Dry Soils. *Soils and Foundations,* **37***,* 3, pp. 95-105 (1997).
[13] PECKER, A., SALENÇON, J. Seismic bearing capacity of shallow strip foundations on clay soils. *Proceedings of International Workshop on Seismology and Earthquake Engineering*. Mexico City, 22-26 April 1991. CENAPRED Mexico City, pp. 287-304 (1991).
[14] PUZRIN, A. M., RANDOLPH, M. F. Generalized Framework for Three - Dimensional Upper bound Limit analysis in a Tresca Material. *ASME, Journal of Applied Mechanics,* **70**, 1, pp. 91-100 (2003).
[15] PUZRIN, A. M., RANDOLPH, M. F. New planar velocity fields for upper bound limit analysis. *International Journal of Solids and Structures,* **40***,* 13-14, pp. 3603 - 3619 (2003).
[16] RICHARDS, R., JR., ELMS, D., G., BUDHU, M. Seismic bearing capacity and settlements of foundations. *Journal of Geotechnical Engineering ASCE,* **119,** 4, pp. 662-674 (1993).
[17] SALENÇON, J. *Calcul à la rupture et analyse limite*. Presses de l'E.N.P.C., Paris, (1983).
[18] SALENÇON, J. An Introduction to the Yield Design Theory and its applications to soil mechanics. *European Journal of Mechanics, A/Solids,* **9***,* 5, pp. 477-500 (1990).
[19] SALENÇON, J. *Handbook of Continuum Mechanics*. Springer Verlag, Berlin, (2001).
[20] SALENÇON, J. *de l'Élastoplasticité au Calcul à la Rupture*. Éditions de l'École Polytechnique, Palaiseau, (2002).
[21] SALENÇON, J., MATAR, M. Capacité portante des fondations superficielles circulaires, *Journal de Mécanique théorique et appliquée,* **1***,* 2*,* pp. 237-267 (1982).
[22] SALENÇON, J., PECKER, A**.** Ultimate Bearing Capacity of shallow foundations under inclined and eccentric loads. Part I: Purely Cohesive Soil. *European Journal of Mechanics, A/Solids,* **14***,* 3, pp. 349-375, (1995).
[23] SALENÇON, J., PECKER, A. Ultimate Bearing Capacity of shallow foundations under inclined and eccentric loads. Part II: Purely Cohesive soil without tensile strength. *European Journal of Mechanics, A/Solids,* **14***,* 3, pp. 377-396 (1995).
[24] SEKIGUCHI, H., KOBAYASHI, S**.** Limit analysis of bearing capacity for a circular footing subjected to eccentric loadings. *Proceedings of the 14th ICSMFE, Hambourg Germany, 1997*, **2**, pp. 1029-1032 (1997).
[25] SARMA S., K., IOSSIFELIS, I. S. Seismic bearing capacity factors of shallow strip footings. *Géotechnique,* **40,** pp. 265-273 (1990).
[26] ZENG, X., STEEDMAN, R. S**.** Bearing capacity failure of shallow foundations in earthquakes. *Géotechnique,* **48**, 2, pp. 235-256 (1998).